

# Diachronous exhumation of HP–LT metamorphic rocks from south-western Alps: evidence from fission-track analysis

S. Schwartz,<sup>1</sup> J. M. Lardeaux,<sup>2</sup> P. Tricart,<sup>3</sup> S. Guillot<sup>3</sup> and E. Labrin<sup>3</sup>

<sup>1</sup>LIRIGM, Université Joseph Fourier, BP 53, 38041 Grenoble Cedex, France; <sup>2</sup>UMR Géosciences Azur, Université Nice Sophia-Antipolis, Nice, France; <sup>3</sup>LGCA-CNRS, Université Joseph Fourier, BP 53, 38041 Grenoble Cedex, France

## ABSTRACT

New fission-track ages on zircon and apatite (ZFT and AFT) from the south-western internal Alps document a diachronous cooling history from east to west, with cooling rates of 15–19 °C Ma<sup>-1</sup>. In the Monviso unit, the ZFT ages are 19.6 Ma and the AFT ages are 8.6 Ma. In the eastern Queyras, ZFT ages range from 27.0 to 21.7 Ma and AFT ages from 14.2 to 9.4 Ma. In the western Queyras, ZFT ages are between 94.7 and 63.1 Ma and AFT ages are between 22.2 and 22.6 Ma. The

Chenaillet ophiolite yields ages of 118.1 Ma on ZFT and 67.9 Ma on AFT. The combination of these new FT data with the available petrological and geochronological data emphasize an earlier exhumation in subduction context before 30 Ma, then in collision associated with westward tilting of the Piedmont zone.

Terra Nova, 19, 133–140, 2007

## Introduction

Geochronological data combined with *P–T* estimates provide information relating to exhumation of high-pressure low-temperature (HP–LT) metamorphic rocks. In the Alpine belt, fission-track (FT) data have mostly been obtained in the central, eastern and north-western domains (Hunziker *et al.*, 1992; Seward and Mancktelow, 1994; Fügenschuh and Schmid, 2003; Malusà *et al.*, 2005). There are very few reliable age data from the Piedmont zone of the south-western Alps (e.g. Carpena and Caby, 1984). The aim of this paper was to present new apatite FT (AFT) and zircon FT (ZFT) data from meta-ophiolites and related meta-sediments in the blueschist and eclogite units from the Piedmont zone of the south-western Alps (Fig. 1). These new data combined with petrological data constrain the exhumation processes in the western Alps.

## Geological setting

The Piedmont zone of the south-western Alps represents the domains juxtaposed during subduction and

Correspondence: Dr Stéphane Schwartz, Université Joseph Fourier, LIRIGM, rue de la Piscine BP53, Maison des géosciences, Grenoble, Rhône-Alpes, 38041 Cedex, France. Tel.: +33 476 82 80 54; fax: +33 476 82 80 70; e-mail: stephane.schwartz@ujf-grenoble.fr

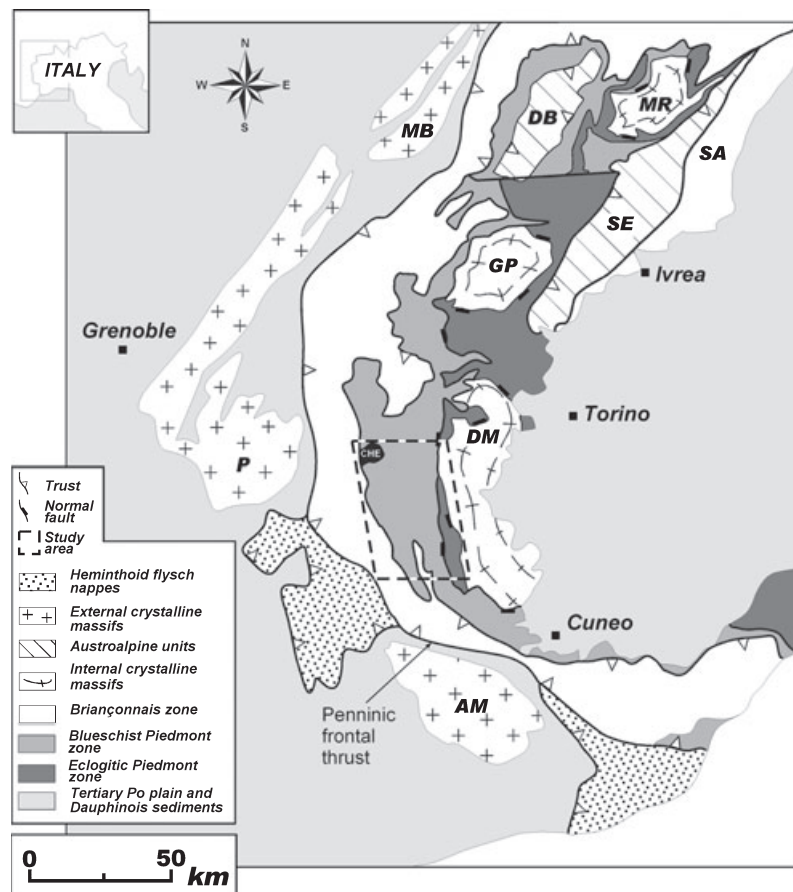


**Fig. 1** Simplified tectonic map of the western Alps, with Argentera-Mercantour (AM), Pelvoux (P), Mont Blanc (MB), Sesia (SE), South-Alpine zone (SA), Dent Blanche (DB), Dora-Maira (DM), Gran-Paradiso (GP), Monte-Rosa (MR), Chenaillet ophiolite (CHE).

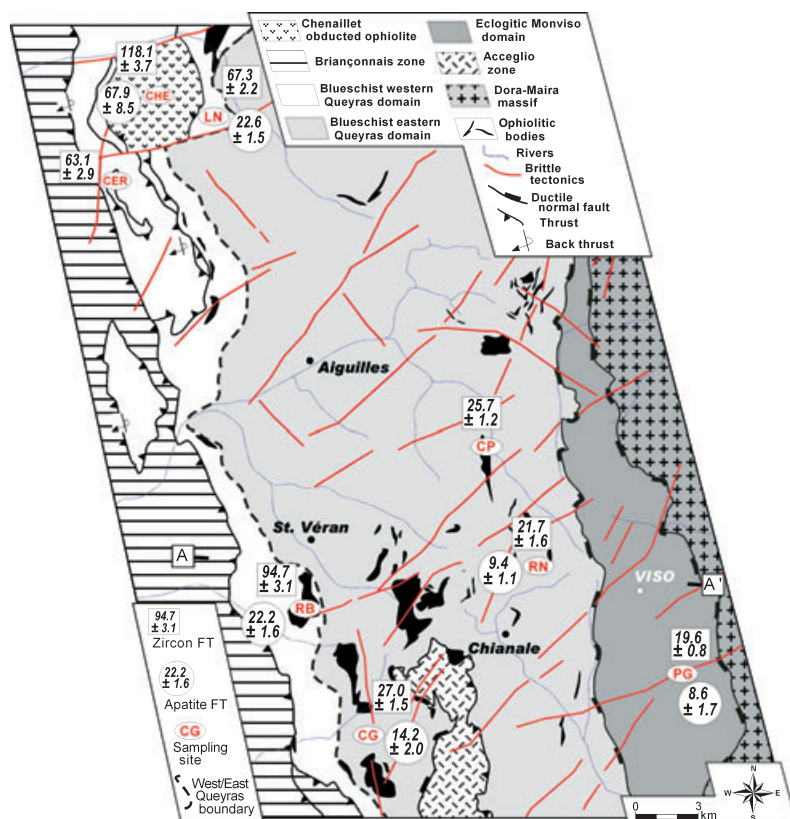


**Fig. 2** The new thermochronological apatite and zircon fission-track ages presented in the studied area, from north to south, Chenaillet ophiolite (CHE), Lago Nero (LN), Cervières (CER), Casse de Peyroun (CP), Rocca Nera (RN), Rocher Blanc (RB), Passo Gallarino (PG), Cirque de la Gavie (CG). A–A' line locates the cross-section in Fig. 4.

collision in Late Cretaceous to Tertiary times (Tricart, 1984; Spalla *et al.*, 1996). Three ophiolite-bearing units are exposed from west to east (Fig. 2). At the top of the nappe pile, the Chenaillet massif represents an obducted portion of the Tethyan oceanic crust, escaping alpine metamorphism. This unit rests upon the Queyras 'Schistes lustrés' complex composed of kilometric scale slices of meta-ophiolites embedded within Mesozoic meta-sedimentary rocks (Lemoine and Tricart, 1986). This unit shows increasing  $P$ – $T$  conditions towards east, with LT-blueschist facies conditions in western Queyras up to the transitional condition between blueschist and eclogite facies in eastern Queyras (Caby, 1996; Schwartz *et al.*, 2000; Agard *et al.*, 2001). The blueschist units are structurally above the eclogitic Monviso ophiolites and the HP to UHP Dora-Maira internal crystalline massif (Fig. 2). In the Monviso massif, the meta-sedimentary compo-

nent is very small (< 20 vol.%) relative to voluminous oceanic lithosphere (Schwartz *et al.*, 2001). Eclogitic metabasals occurred as boudins in a matrix of serpentinites or highly deformed meta-basalts. The calculated  $P$ – $T$  conditions are heterogeneous among different boudins, suggesting that different fragments correspond to oceanic slab subducted to different depths (Blake *et al.*, 1995; Schwartz *et al.*, 2001).

## FT methods and results

### FT analytical procedures

Zircons and apatites were separated using conventional rock-crushing, heavy liquids, Frantz magnetic separator and hand picking. Polishing and etching procedures were those recommended by Hurford (1990). All samples were analysed by the external detector method (Gleadow, 1981) which allowed the uranium concen-

tration and age for individual crystals to be determined. Prior to irradiation, all zircons were etched using the KOH–NaOH eutectic at 220 °C for 15 h (Gleadow *et al.*, 1976) and all apatites were etched with 1 N HNO<sub>3</sub> at 20 °C for 50 s. Samples were irradiated at the Orphée reactor (Centre d'Etudes Nucléaires, Saclay, France). Neutron fluences were monitored using uranium glass dosimeters (CN-1 for zircon and CN-5 for apatite). Ages were calculated using the zeta calibration approach, whereby a proportionality constant zeta is evaluated by multiple analyses of mineral standards of known age (Hurford and Green, 1983). Zeta values used in this study have been determined from repeated measurements of standard zircons from the Fish Canyon Tuff (USA) and standard apatites from the Durango deposit (Mexico). The ages presented correspond to the central ages following Galbraith (1992). These central ages are modal ages, weighted to account for the differing precision of the individual crystal age. Two uncertainties are related to the central age: the  $\pm$  indicates the analytical precision, while an estimate of the age dispersion (or the spread of the individual crystal data) is given by the relative standard error of the central age (RE).

### The Chenaillet unit

Amphibolite to prehnite–pumpellyite facies conditions, representing the metamorphism on the ocean floor, have been recognized by Mével *et al.* (1978). Fourteen grains of zircons from an albitite dyke cross-cutting the serpentinitized mantle peridotites (Tables 1 and 2) yielded a central age of 118  $\pm$  3.7 Ma. The individual age dispersion is low (relative error of central age: RE < 1%), from 86.6 to 142.5 Ma, with a  $\chi^2$  test higher than 90% (Fig. 3a). For apatites, a central age of 67.9  $\pm$  8.5 Ma was obtained on nine grains. Despite their low uranium content, these apatites show a very low dispersion of individual ages (RE < 1%) and a  $\chi^2$  test higher than 85%.

### The eclogitic Monviso ophiolites

Forty-three grains of zircon were investigated from the Fe–Ti metabasals of the Passo Gallarino unit

**Table 1** Sample locations and petrological descriptions of rocks used for ZFT and AFT investigations. Elevation is in metres above sea level and geographical coordinates are latitude and longitude.

Sample	Location	Geographical coordinates	Description	Elevation
PG	Passo Gallarino, Monviso Massif	44°38'N, 7°7'E	Centimetric to metric boudins of eclogitic Fe–Ti gabbro. The paragenesis consists of garnet, omphacite, glaucophane, rutile and $\pm$ quartz	2621 m
RN	Rocca Nera, eastern Queyras	44°41'N, 6°59'E	Decimetric interstratified arkosic levels within the calcschists. The rocks have suffered blueschist facies metamorphism with development of jadeite, glaucophane and zoisite	2750 m
CP	Casse de Peyroun, eastern Queyras	44°44'N, 6°59'E	Cement of a magmatic breccia with doleritic elements. The blueschist paragenesis is characterized by development of jadeite, zoisite and glaucophane	1956 m
CG	Cirque de la Gavie, eastern Queyras	44°36'N, 6°54'E	Albitic dykes boudinaged within serpentinites. The rock shows the association of albite, lawsonite (80%) and glaucophane developed during blueschist facies Alpine metamorphism	2700 m
RB	Rocher Blanc, western Queyras	44°40'N, 6°52'E	Polygenic breccia with predominant granitoid elements and subordinated metabasalt elements. The rock has recrystallized under blueschist facies conditions during Alpine metamorphism. The paragenesis consists of jadeite, lawsonite, phengite and glaucophane	2700 m
LN	Lago Nero, western Queyras	44°53'N, 6°47'E	Breccia formed with detrital material of continental origin. The rock is composed of quartz, jadeite and phengite developed during blueschist facies Alpine metamorphism	2030 m
CER	Cervières, western Queyras	44°53'N, 6°44'E	Breccia formed with detrital material of continental origin. The rock consists of quartz, jadeite and phengite	1630 m
CHE	Chenaillet massif	44°53'N, 6°44'E	Leucocratic zones cross-cutting serpentinites. Greenschist facies assemblage is related to the oceanic metamorphism	2600 m

(Table 1), which records the peak metamorphic condition of  $450 \pm 50$  °C and 13–15 kbar (Schwartz *et al.*, 2000). The data have low relative errors (RE < 1%) and high score of the  $\chi^2$  test (value > 99%) yielding an age of

$19.6 \pm 0.8$  Ma (Table 2 and Fig. 3d). In the case of apatites, 23 crystals, all with low uranium content have been dated. However, all ages are in a range from 14.0 to 6.1 Ma, with a central age of  $8.6 \pm 1.7$  Ma (RE < 1%) (Figs 2 and 3d).

#### The blueschist eastern Queyras domain

The  $P$ – $T$  conditions in the meta-gabbros have been estimated at 350–450 °C for a minimum pressure of 9 kbar (Caby, 1996; Schwartz, 2002), compatible with the development of

**Table 2** Fission-track data measured for the Piedmont zone of the south-western Alps. Track densities ( $\rho$ ) ( $\times 10^5$  tracks  $\text{cm}^{-2}$ ), number of tracks counted ( $n$ ) shown in brackets. All analyses by external detector method use 0.5 as  $4\pi/2\pi$  geometry correction factor.  $P\chi^2$  is the probability of obtaining  $\chi^2$  value for  $\nu$  degrees of freedom (where  $\nu$  = number of crystals – 1). RE is the relative error of central age. In our results the dispersion is always low (< 10%) leading to the recognition of a single age population. All uncertainties are quoted at  $1\sigma$  level.

Sample	Mineral	Number of crystals	Spontaneous $\rho_s$ (Ns)	Induced $\rho_i$ (Ni)	$P\chi^2$ (%)	RE (%)	Dosimeter $\rho_d$ (Nd)	Zeta ( $\pm\sigma$ )	Age $\pm 1\sigma$ (Ma)
Monviso eclogitic domain									
PG	Apatite	23	0.049 (28)	1.59 (914)	>99	<1	19.39 (15 899)	$289 \pm 13$	$8.6 \pm 1.7$
	Zircon	43	2.43 (764)	2.25 (709)	>99	<1	2.90 (10 734)	$125 \pm 3$	$19.6 \pm 0.8$
Eastern Queyras blueschist domain									
RN	Apatite	14	0.810 (94)	24.03 (2786)	>99	<1	19.39 (15 899)	$289 \pm 13$	$9.4 \pm 1.1$
	Zircon	3	39.40 (164)	23.30 (97)	56	<1	2.05 (10 854)	$125 \pm 3$	$21.7 \pm 1.6$
CP	zircon	15	5.27 (489)	2.64 (245)	>99	<1	2.05 (10 854)	$125 \pm 3$	$25.7 \pm 1.2$
CG	Apatite	31	0.255 (57)	5.01 (1120)	>99	<1	3.37 (9090)	$289 \pm 13$	$14.2 \pm 2.0$
	Zircon	19	1.80 (285)	1.21 (192)	>99	<1	2.90 (10 734)	$125 \pm 3$	$27.0 \pm 1.5$
Western Queyras blueschist domain									
RB	Apatite	26	1.32 (263)	2.87 (574)	>99	<1	3.37 (9090)	$289 \pm 13$	$22.2 \pm 1.6$
	Zircon	12	73.00 (2532)	9.86 (342)	95	<1	2.05 (10 854)	$125 \pm 3$	$94.7 \pm 3.1$
LN	Apatite	14	4.62 (374)	9.92 (803)	>99	<1	3.37 (9090)	$289 \pm 13$	$22.6 \pm 1.5$
	Zircon	11	72.50 (2425)	13.80 (462)	>99	<1	2.05 (10 854)	$125 \pm 3$	$67.3 \pm 2.2$
CER	Zircon	2	165.00 (423)	33.60 (86)	70	<1	2.05 (10 854)	$125 \pm 3$	$63.1 \pm 2.9$
Chenaillet massif without alpine metamorphism									
CHE	Apatite	9	0.958 (57)	2.00 (119)	87	<1	9.88 (10 454)	$289 \pm 13$	$67.9 \pm 8.5$
	Zircon	14	80.50 (3385)	8.70 (366)	92	<1	2.05 (10 854)	$125 \pm 3$	$118.1 \pm 3.7$
									$118.1 \pm 3.7$

chloritoid–phengite assemblage in the metapelites (Agard *et al.*, 2001). The zircon central ages are  $27.0 \pm 1.5$  Ma in the Cirque de la Gavie,  $25.7 \pm 1.2$  Ma in the Casse de Peyroun area and  $21.7 \pm 1.6$  Ma in the Rocca Nera area (Fig. 2). All zircons have a small dispersion of the individual crystal ages, with the RE always lower than 1% and a high  $\chi^2$  test (Fig. 3c). However, in the case of Rocca Nera, the  $\chi^2$  is lower (value > 55%) than in the other localities because of the low number of induced and spontaneous counted tracks (Table 2). The apatite central ages are younger than the zircon central ages with ages of  $14.2 \pm 2.0$  Ma in the Cirque de la Gavie area and of

$9.4 \pm 1.1$  Ma in the Rocca Nera area (Fig. 2). The AFT results show a low dispersion of the individual crystal ages (RE < 1%), but their central ages are always lower than the zircon central ages always obtained in the same locality (Fig. 3c).

**The blueschist western Queyras domain**

This domain corresponds to the westernmost part of the Piedmont zone (Fig. 2). *P–T* is estimated at 8–10 kbar for 300–350 °C in the metagabbros (Caby, 1996; Schwartz, 2002), consistent with the development of carpholite in metapelites (Agard *et al.*, 2001). Five ages were obtained, two

on apatites giving rise to homogeneous results around 22 Ma, and three on zircons with ages strongly varying between  $63.1 \pm 2.9$  Ma (Cervières area) and  $94.7 \pm 3.1$  Ma (Rocher Blanc area) (Fig. 3b).

The ZFT ages have a very low dispersion for the individual crystal ages and a high  $\chi^2$  value (Fig. 3b). In the sample from the Cervières area, ages were obtained only from two crystals of zircon, but the high density of induced and spontaneous tracks allows to calculate a central age of  $63.1 \pm 2.9$  Ma. These zircon ages are significantly older than the ages obtained by the same technique for the easternmost domains. Apatite ages have been obtained only for Rocher

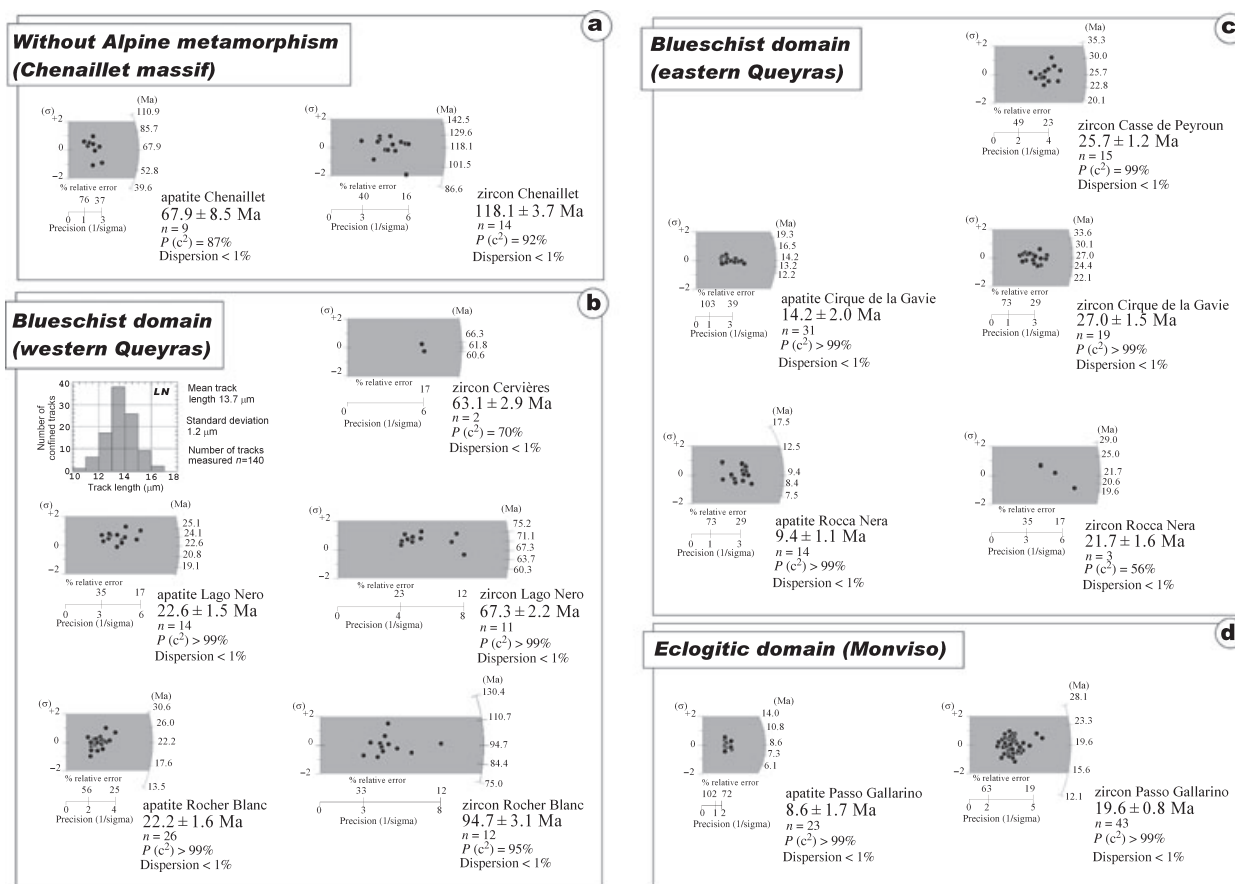


**Fig. 3** Radial plots of apatite and zircon ages for the different metamorphic domains of the Piedmont zone. The count data are presented using the radial plot of Galbraith (1990), corresponding to a graphical device for comparing crystals of differing ages and differing precisions. The position of the *x* scale records the uncertainty of grain estimates depending on the density counted tracks, whilst each point has the same standard error in the *y* direction (indicated by the vertical +2 to –2 bar). The plot also includes a circular age scale such that the age of any crystal may be determined by extrapolating a line from the origin through the crystal’s *x,y* coordinates to intercept the age scale. For the Lago Nero unit (LN) the apatite track-length measurements are presented. These data are displayed as a histogram with individual measurements grouped in 1 µm bins. The number of tracks in each bin is represented on the *y* axis.



Blanc and Lago Nero areas. In both cases, the individual age dispersion is low ( $RE < 1\%$ ) and the  $\chi^2$  value is high ( $> 90\%$ , Table 2). The central ages are compatible at about 22 Ma (Fig. 3b). In the case of the Lago Nero apatites, high uranium content allowed the measurement of confined track lengths (Fig. 3b). The track length distribution defines a symmetrical shape centred on  $13.5 \pm 1.2 \mu\text{m}$  compatible with a constant and progressive cooling of the sample through the partial retention zone (Dumitru, 1989).

### FT interpretation

The FT data from both zircons and apatites represent single cooling ages, i.e. single populations (Fig. 3). In the case of rapid cooling rate ( $> 10 \text{ }^\circ\text{C Ma}^{-1}$ ), AFT closure temperature is of about  $110 \pm 10 \text{ }^\circ\text{C}$  (e.g. Reiners and Brandon, 2006). The zircon samples from the Queyras wedge have a low U content (Carpéna and Caby, 1984; Schwartz, 2002), susceptible to generate low  $\alpha$ -decay damage density and high resistance to FT annealing. In this case, the maximum temperature recorded by the ZFT are nearby  $340 \text{ }^\circ\text{C}$ , which corresponds to the upper limit of the partial annealing zone predicted from low to zero-damage models (Yamada *et al.*, 1995; Rahn *et al.*, 2004). Thus, according to Reiners and Brandon (2006), we consider a closure temperature of  $300 \pm 40 \text{ }^\circ\text{C}$  for ZFT.

The FT age data are summarized as follows:

- the Chenaillet massif was not affected by alpine metamorphism. Even the low-temperature metamorphism (greenschist facies and prehnite–pumpellyite facies) must be older than 65 Ma, suggesting that the ophiolite was obducted before 65 Ma;
- Monviso and eastern Queyras reveal progressively older ages towards the west and tectonic upper levels (Fig. 4). However, combining zircon and apatite ages yields similar mean cooling rate of  $15\text{--}19 \text{ }^\circ\text{C Ma}^{-1}$  (Fig. 4);
- in western Queyras, the AFT ages are similar, around 22 Ma, whereas zircon ages vary widely. The wide variation in zircon ages is explained by low temperature metamorphic

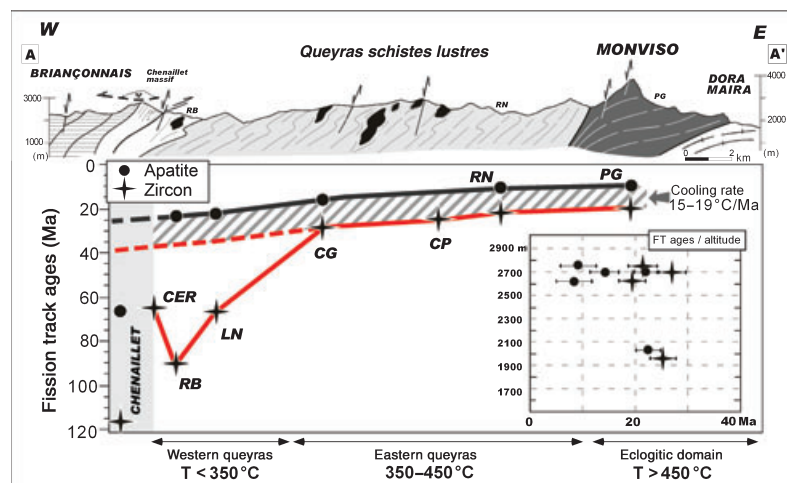


**Fig. 4** Cooling rates for the different tectono-metamorphic units presented on a cross-section of the study area (A–A' transect in Fig. 2). See Fig. 2 for the FT sample sites abbreviations. The distribution of the cooling ages supports diachronous histories for the different units. The extrapolation of the trend obtained in the eastern part probably suggests that the western Queyras cooled below  $300 \text{ }^\circ\text{C}$  between 39 and 31 Ma. The ZFT and AFT ages are plotted in age/altitude diagram (we do not report ZFT data from the Chenaillet and the western Queyras). There is no clear correlation between the calculated ages and the altitudes, which suggests that the Piedmont zone was not exhumed as a single crustal unit.

condition ( $T < 350 \text{ }^\circ\text{C}$ ), which is close to the FT annealing temperature of zircon ( $340 \text{ }^\circ\text{C}$ ), and is too low for resetting ZFT (Brix *et al.*, 2002). Thus, these ages have no geological significance. The extrapolation of the trend obtained for the ZFT ages towards the west suggests that the western Queyras possibly cooled below  $300 \text{ }^\circ\text{C}$  between 39 and 31 Ma (Fig. 4);

- the cooling histories of different ophiolite-bearing metamorphic units are diachronous. The easternmost eclogitic units cooled later and thus exhumed later than the westernmost blueschist units.

### Alpine temperature–time paths

In the south-western Alps, subduction processes are mainly recorded by the development of a regional HP–LT metamorphism dated between 50 and 45 Ma in meta-ophiolites of the Monviso Massif (Monié and Philippot, 1989; Duchêne *et al.*, 1997b; Cliff *et al.*, 1998; Rubatto and Hermann, 2001), and at around 35–32 Ma in the Dora-Maira massif (Tilton *et al.*, 1989, 1991; Duchêne *et al.*, 1997a,b; Gebauer *et al.*, 1997; Di Vincenzo

*et al.*, 2006). The transition from subduction to collision dynamics occurred at about 30–34 Ma and is marked by the activation of the Penninic frontal thrust and the onset of exhumation of the Dora-Maira massif (Ford *et al.*, 2006). Our data clearly refer to the post-collisional history of the south-western Alps. The obtained  $T$ – $t$  paths show a diachroneity in the cooling history of a minimum of 5 Ma between the three studied units (Fig. 5). The western Queyras was first cooled followed by the cooling of eastern Queyras and Monviso massif. The similar cooling paths for the three units suggest that they were exhumed by the similar process but not at the same time. Moreover, two periods of cooling are distinguished (Fig. 5):

- between 300 and  $110 \text{ }^\circ\text{C}$ , the Monviso massif cooled more rapidly than the Queyras units  $19$  and  $15 \text{ }^\circ\text{C Ma}^{-1}$ , respectively. This suggests that the thermal behaviour of the eastern and western Queyras is similar while the Monviso unit is distinct;
- between  $110 \text{ }^\circ\text{C}$  up to the surface, the cooling rates slightly decrease but also spatially from east to west (from  $12$  to  $5 \text{ }^\circ\text{C Ma}^{-1}$ ). This sug-

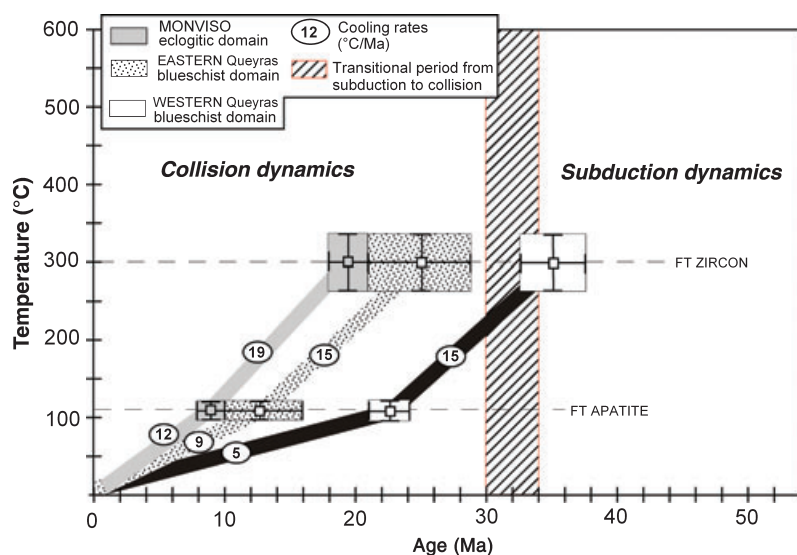


**Fig. 5** Temperature–time paths for Monviso, western and eastern Queyras established by ZFT and AFT data. Cooling rates are also indicated for each unit.

gests that during the final exhumation, the thermal behaviour of the three units was different.

**Tectonic consequences and discussion**

**Arguments for a Palaeocene to Eocene intra-oceanic subduction zone**

Our data are consistent with an intra-oceanic subduction zone for the Alpine Piedmont zone (Fig. 6). It is difficult to estimate the location of Chenaillet ophiolite in the Piedmont oceanic domain, but it has remained in the upper tectonic position. Emplacement of the Chenaillet unit

onto the European margin could have occurred between upper Cretaceous and Eocene. During the Palaeocene or Eocene, the Piedmont zone was metamorphosed under blueschist facies conditions in a sedimentary accretionary wedge, while the eclogitized meta-ophiolites represent pieces of the subducted oceanic lithosphere. During active subduction, pieces of eclogites were exhumed in a serpentinized subduction channel (Hermann *et al.*, 2001; Schwartz *et al.*, 2001). This sedimentary serpentinized subduction was stacked at the base of the sedimentary accretionary wedge (Fig. 6) as proposed by Schwartz *et al.* (2000).

**Continental subduction**

The UHP metamorphism in the Dora-Maira massif occurred at about 31–35 Ma as previously discussed. Considering this massif as a remnant of the European continental margin, the continental subduction started prior Oligocene time. A low convergence rate, of about 6–8 mm yr<sup>-1</sup>, between Africa and Europe from Late Cretaceous to Eocene (Jolivet and Faccenna, 2000; Schettino and Scotese, 2002) suggests a minimum of 17 Ma for the Dora-Maira massif to reach the depth of 120 km recorded by the UHP metamorphism. This implies that continental subduction was probably initiated before 45–50 Ma in the south-western Alps, i.e. at the time of the HP metamorphism in the Monviso ophiolites. Thus, we propose that the onset of exhumation of the Piedmont zone is broadly contemporaneous with the initial continental subduction of the Dora-Maira massif. The contrasted cooling rates of the Queyras Schistes lustrés and the Monviso after 30 Ma is thus synchronous with the onset of exhumation of the Dora-Maira massif.

**Arguments for tectonic decoupling in the Piedmont zone**

The Schistes lustrés and Monviso unit are separated by a ductile normal fault (Ballèvre *et al.*, 1990). Our chronological data are compatible with this tectonic observation. Moreover, after 22 Ma, the western Queyras started to cool more slowly than the eastern Queyras and the Monviso units (Fig. 5). This can be related to the onset of westward tilting of the units in response to the upward indentation of the Dora-Maira massif as recently proposed by Tricart *et al.* (2004).

**Conclusions**

Coupled FT analysis on zircons and apatites from meta-ophiolites of the Piedmont zone documents diachronous cooling histories and related to contrasted exhumation history.

Three tectonic domains likely represent remnants of three different structural levels of the same palaeo-subduction zone. (i) The highest structural level corresponds to the Chenaillet unit as obducted upon the

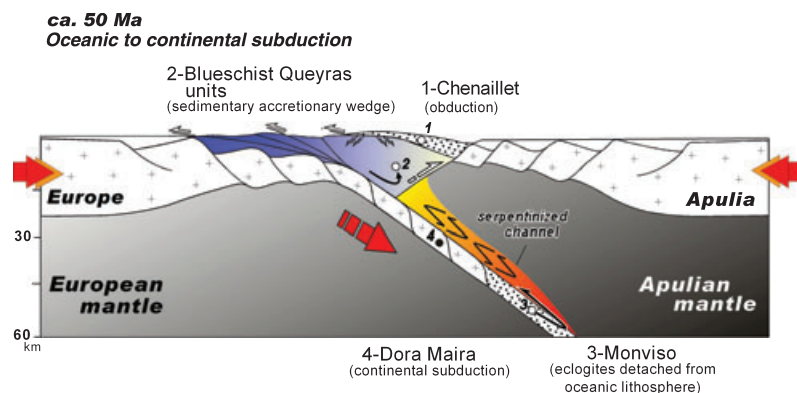


**Fig. 6** Tectonic sketch of the Piedmont zone during the Eocene. The different metamorphic domains that presently outcrop in the Piedmont zone ‘sample’ different levels of a palaeo-subduction zone.

European margin before 65 Ma. (ii) The blueschist Queyras units (eastern and western Queyras) correspond to the deformed sedimentary accretionary wedge, while (iii) the Monviso eclogitic units represent the subducted oceanic slab, exhumed in a serpentinite channel and then stacked at the base of the sedimentary accretionary wedge. We quantified the final exhumation of the Monviso and Queyras units which occurred during the post-collision history of the studied area. This exhumation is diachronous (19 and 35 Ma for ZFT, 9 and 22 Ma for AFT) and confirms the existence of the tectonic decoupling inside the Piedmont zone.

### Acknowledgements

The authors are grateful to K. Hattori, D. Seward, L. Jolivet, M. Zattin and I. Villa for their helpful comments. We thank G. Poupeau for fission-tracks laboratory facilities. This work was supported by the CNRS-BRGM program 'Geo-France 3D – Alpes'.

### References

- Agard, P., Jolivet, L. and Goffé, B., 2001. Tectonometamorphic evolution of the Schistes lustrés complex: implications for the exhumation of HP and UHP rocks in the western Alps. *Bull. Soc. Géol. Fr.*, **5**, 604–617.
- Ballèvre, M., Lagabrielle, Y. and Merle, O., 1990. Tertiary ductile normal faulting as a consequence of lithospheric stacking in the Western Alps. *Soc. Géol. Fr. Mem.*, **156**, 227–236.
- Blake, M.C., Moore, D.E. and Jayko, A.S., 1995. The role of the serpentinite melange in the unroofing of UHP metamorphic rocks: an example from western Alps of Italy. In: *Ultrahigh Pressure Metamorphism* (R.G. Coleman and X. Wang, eds), pp. 182–205. Cambridge University Press, London.
- Brix, M.R., Stöckhert, B., Seidel, E., Theye, T., Thomson, S.N. and Küster, M., 2002. Thermobarometric data from a fossil zircon partial annealing zone in high pressure–low temperature rocks of eastern and central Crete, Greece. *Tectonophysics*, **349**, 309–326.
- Caby, R., 1996. Low-angle extrusion of high-pressure rocks and the balance between outward and inward displacements of middle penninic units in the western Alps. *Eclogae Geol. Helv.*, **89/1**, 229–267.
- Carpéna, J. and Caby, R., 1984. Fission-track evidence for late Triassic oceanic crust in French occidental Alps. *Geology*, **12**, 108–111.
- Cliff, R.A., Barnicoat, A.C. and Inger, S., 1998. Early Tertiary eclogite facies metamorphism in the Monviso Ophiolite. *J. Metamorph. Geol.*, **16**, 447–455.
- Di Vincenzo, G., Tonarini, S., Lombardo, B., Castelli, D. and Ottolini, L., 2006. Comparison of  $^{40}\text{Ar}$ – $^{39}\text{Ar}$  and Rb–Sr data on phengites from the UHP Brossasco-Isasca unit (Dora Maira Massif, Italy): implications for dating white mica. *J. Petrol.*, **47**, 1439–1465.
- Duchêne, S., Lardeaux, J.M. and Albarède, F., 1997a. Exhumation of eclogites: Insights from retrograde depth-time path analysis. *Tectonophysics*, **280**, 125–140.
- Duchêne, S., Blichert-Toft J., Luais, B., Télouk, P., Lardeaux, J.M. and Albarède, F., 1997b. The Lu–Hf dating of the garnets and the ages of the Alpine high-pressure metamorphism. *Nature*, **387**, 586–589.
- Dumitru, T.A., 1989. Constraints on uplift in the Franciscan subduction complex from apatite fission-track analysis. *Tectonics*, **8**, 197–220.
- Ford, M., Duchêne, S., Gasquet, D., Vanderhaeghe, O., 2006. Two-phase orogenic convergence in the external and internal SW Alps. *J. Geol. Soc. London*, **163**, 1–12.
- Fügenshuh, B. and Schmid, S.M., 2003. Late stages of deformation and exhumation of an orogen constrained by fission-track data: a case study in Western Alps. *Geol. Soc. Am. Bull.*, **115**, 1425–1440.
- Galbraith, R.F., 1990. The radial plot: graphical assessment of spread in ages. *Nucl. Tracks*, **17**, 207–214.
- Galbraith, R.F., 1992. Statistical models for mixed ages. *Abstracts with programs, 7th International Workshop on Fission-track Thermochronology, University of Pennsylvania*, July 1992, p. 7.
- Gebauer, D., Schertl, H.P., Brix, M. and Schreyer, W., 1997. 35 Ma old ultrahigh-pressure metamorphism and evidence for very rapid exhumation in the Dora-Maira massif, Western Alps. *Lithos*, **41**, 5–24.
- Gleadow, A.J.W., 1981. Fission-track dating methods: what are the real alternatives? *Nucl. Tracks*, **5**, 3–14.
- Gleadow, A.J.W., Hurford, A. and Quaipe, D.R., 1976. Fission-track dating of zircon-improved etching techniques. *Earth Planet. Sci. Lett.*, **33**, 273–276.
- Hermann, J., Müntener, O. and Scambelluri, M., 2001. The importance of serpentinite mylonites for subduction and exhumation of oceanic crust. *Tectonophysics*, **327**, 225–238.
- Hunziker, J.C., Desmons, J. and Hurford, A., 1992. Thirty-two years of geochronological work in the Central and Western Alps: a review on seven maps. *Mém. Géol. Lausanne*, **13**, 59.
- Hurford, A., 1990. International Union of Geophysical Sciences subcommission on geochronology recommendation for standardization of fission-track dating calibration and data reporting. *Nucl. Tracks*, **2**, 233–236.
- Hurford, A. and Green, P.F., 1983. The zeta age calibration of fission-track dating. *Isotope Geosci.*, **1**, 285–317.
- Jolivet, L. and Faccenna, C., 2000. Mediterranean extension and the Africa–Eurasia collision. *Tectonics*, **19**, 1095–1106.
- Lemoine, M. and Tricart, P., 1986. Les Schistes lustrés des Alpes occidentales: approche stratigraphique, structurale et sédimentologique. *Eclogae Geol. Helv.*, **79**, 271–294.
- Malusà, G., Polino, R., Zattin, M., Bigazzi, G., Martin, S. and Piana, F., 2005. Miocene to Present differential exhumation in Western Alps: insights from fission track thermochronology. *Tectonics*, **24**, 1–23.
- Mével, C., Caby, R. and Kienast, J.R., 1978. Amphibolite facies conditions in oceanic crust: example of amphibolitized flaser gabbros and amphibolites from the Chenaillet ophiolite massif (Hautes Alpes, France). *Earth Planet. Sci. Lett.*, **39**, 98–108.
- Monié, P. and Philippot, P., 1989. Mise en évidence de l'âge Eocène moyen du métamorphisme de haute-pression de la nappe ophiolitique du Mont Viso (Alpes occidentales) par la méthode  $^{39}\text{Ar}/^{40}\text{Ar}$ . *CR Acad. Sci. Paris*, **309**, 245–251.
- Rahn, M., Brandon, M., Batt, G. and Garver, J., 2004. A zero-damage model for fission track annealing in zircon. *Am. Miner.*, **89**, 473–484.
- Reiners, P.W. and Brandon, M.T., 2006. Using thermochronology to understand orogenic erosion. *Annu. Rev. Earth Planet. Sci.*, **34**, 419–466.
- Rubatto, D. and Hermann, J., 2001. Exhumation as fast as subduction? *Geology*, **29**, 3–6.
- Schettino, A. and Scotese, C., 2002. Global kinematic constraints to the tectonic history of the Mediterranean region and surrounding areas during the Jurassic to the Cretaceous. *J. Virtual Explorer*, **8**, 145–160.
- Schwartz, S., 2002. La zone Piémontaise des Alpes occidentales: un paléo-complexe de subduction. Arguments métamorphiques, géochronologiques et structuraux. *Documents BRGM Orléans*, **302**, 313.
- Schwartz, S., Lardeaux, J.M., Guillot, S. and Tricart, P., 2000. Diversité du métamorphisme eclogitique dans le massif ophiolitique du Monviso (Alpes Occidentales, Italie). *Geodin. Acta*, **13**, 169–188.

- Schwartz S., Allemand P. and Guillot S., 2001. Numerical model of the effect of serpentinites on the exhumation of eclogitic rocks: insights from the Monviso ophiolitic massif (western Alps). *Tectonophysics*, **342**, 193–206.
- Seward, D. and Mancktelow, N. S., 1994. Neogene kinematics of central and western Alps: evidence from fission-track dating. *Geology*, **22**, 803–806.
- Spalla, M.I., Lardeaux, J.M., Dal Piaz, G.V., Gosso, G. and Messiga, B., 1996. Tectonic significance of alpine eclogites. *J. Geodyn.*, **21**, 257–285.
- Tilton, G.R., Schreyer, W. and Schertl, H.P., 1989. Pb–Sr–Nd isotopic behavior of deeply subducted crustal rocks from the Dora-Maira Massif, Western Alps, Italy. *Geochim. Cosmochim. Acta*, **53**, 1391–1400.
- Tilton, G.R., Schreyer, W. and Schertl, H.P., 1991. Pb–Rb–Nd isotopic behaviour of deeply subducted crustal rocks from the Dora-Maira massif, western Alps, Italy – II: what is the age of the ultrahigh-pressure metamorphism? *Contrib. Mineral. Petrol.*, **108**, 22–33.
- Tricart, P., 1984. From passive margin to continental collision: a tectonic scenario for the Western Alps. *Am. J. Sci.*, **284**, 97–120.
- Tricart, P., Schwartz, S., Sue, C. and Lardeaux, J.M., 2004. Evidence for synextensional tilting and doming during final exhumation from analysis multistage faults (Queyras, Schistes lustrés, Western Alps). *J. Struct. Geol.*, **26**, 1633–1645.
- Yamada, R., Tagami, T., Nishimura, S. Ito, H., 1995. Annealing kinetics of fission-tracks in zircon: an experimental study. *Chem. Geol.*, **122**, 249–258.

Received 11 April 2006; revised version accepted 22 November 2006